



CHORUS

This is the accepted manuscript made available via CHORUS. The article has been published as:

math
xmlns="http://www.w3.org/1998/Math/MathML">msup>mi
> β /mi>mn>2/mn>/msup>/math> corrections to spherical
energy-density functional calculations for root-mean-square
charge radii

B. Alex Brown and Kei Minamisono

Phys. Rev. C **106**, L011304 — Published 20 July 2022

DOI: [10.1103/PhysRevC.106.L011304](https://doi.org/10.1103/PhysRevC.106.L011304)

β^2 corrections to spherical EDF calculations for root-mean-square charge radii

B. Alex Brown and Kei Minamisono¹

¹*Department of Physics and Astronomy, FRIB Laboratory,
Michigan State University, East Lansing, MI 4284-1321, USA*

(Dated: June 16, 2022)

Root-mean-square charge radii are discussed in terms of spherical Energy Density Functional (EDF) models corrected for quadrupole deformations. We discuss the specific examples for the isotope shifts of the calcium isotopes and the isotonic shift between tin and cadmium.

INTRODUCTION

Root-mean-square (rms) charge radii of nuclei provide one of the most precise insights into nuclear structure. New experiments are being carried out on long chains of isotopes, and theoretical models are being improved, see [1], [2], [3], [4] and references therein. Fig. (1) shows the measured rms charge radii for even-even nuclei from calcium to tellurium. One observes kinks in the isotopic trends at neutron numbers $N = 28$ and $N = 50$, as well as kinks in the isotonic trends at the proton numbers $Z = 28$ and $Z = 50$. To set the scale for understanding the data, we show in Fig. (2) experimental rms charge radii compared to the simple two parameter formula from [5].

One of the most famous and challenging data for rms charge radii is that for the calcium isotopes where, as observed in Figs. (1) and (3), there is a strong odd-even oscillation in the rms charge radii with $^{42,44,46}\text{Ca}$ being relatively large compared to those for the "closed-shell" nuclei ^{40}Ca and ^{48}Ca . It is notable that the experimental rms charge radii of ^{40}Ca and ^{48}Ca are nearly the same [6]. This data has led to many theoretical ideas [7], [8], [9], [10], [11], [12], [13], [14], [15], [16], [17]. It was noted by Zamick [7] and Talmi [9] that a two-body effective operator for a correction to rms radii contains odd-even oscillations.

In the letter, we focus on calculations for the relative charge radii of the calcium isotopes [6], [18] shown in Fig. (3), and the isotopic shift between the charge radii of tin [19] and cadmium [20] (Sn-Cd) shown in Fig. (4). The data are compared to spherical density-functional-theory (DFT) calculations obtained with the Sv-min [21] and Fy(Δr) [3] energy-density functional (EDF) used for comparison in those experimental papers. The Sv-min results for the calcium data do not show the observed oscillations. This result is similar to those obtained in Covariant Density Functional (CODF) models (see Fig. 24 in Ref. [2]). The Sv-min results for the Sn-Cd isotonic shift are too large compared to experiment. The Fy(Δr) results for Ca are in better agreement with the experimental oscillations due to the addition of the Fayans pairing term with a parameter adjusted to fit data for the oscillations including the data for Ca [3]. The Fy(Δr) results for the Sn-Cd isotonic shift do not agree with the

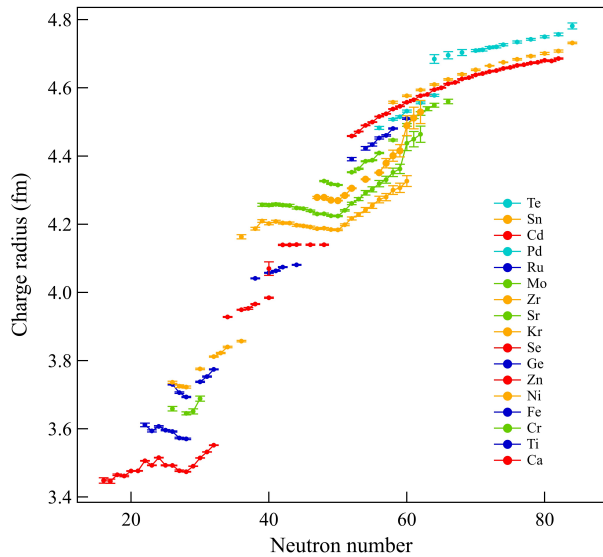


FIG. 1. Measured rms charge radii for nuclei from $Z = 20$ (calcium) to $Z = 52$ (tellurium). The data are taken from compilations [22] and [23] with updated results for Ca [6], [18], Fe [24], Ni [25], Cd [20], and Sn [19].

data.

It is well known that deformation plays a key role in understanding shell effects in the rms radii [26]. The reason is that the deformed intrinsic shape has a larger rms radius compared to the spherical shape. In the deformed Bohr model of an incompressible fluid, the increase in rms radius is connected to the deformation parameter β_2 and to the $B(E2)$ values between the ground state and low-lying states. Usually this is applied to well deformed even-even nuclei. We will show that the Bohr-model equation can be used to describe the rms-radius data for nuclei that are not so well deformed, with the two examples shown in Figs. 3 and 4, by using experimental data for the $B(E2)$ for the even-even nuclei. Furthermore, we will derive a more general result that includes odd-even nuclei. We carry out configuration-interaction calculations for the calcium isotopes that reproduce the experimental $B(E2)$ values for the even-even nuclei. These can also be applied to the odd-even nuclei. The resulting trends in the rms charge radii are in good agreement with

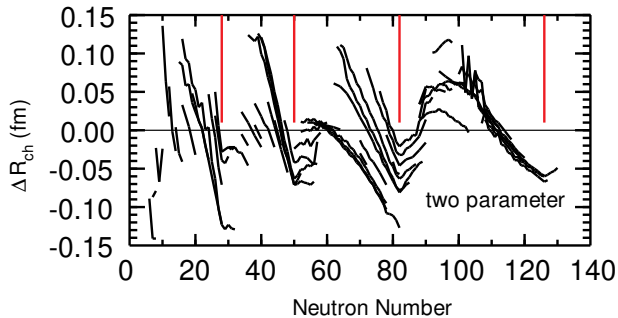


FIG. 2. $\Delta_{ch} = R_{ch}(\text{exp}) - R_{ch}(2p)$ with the two-parameter formula $R_{ch}(2p) = r_0 A^{1/3} + r_1 A^{-1/3}$ with $r_0=0.9071$ fm and $r_1=1.105$ fm from [5].

experiment. In particular, the odd-even oscillations are reproduced. We interpret the oscillation in the effective β_2 values as being due to a blocking effect of the odd neutron.

In the Bohr model of a deformed incompressible fluid with a quadrupole deformation parameter β_2 , one obtains an increase in the mean-square matter radius

$$\langle r^2 \rangle = \langle r^2 \rangle_0 \left[1 + \frac{5\beta_2^2}{4\pi} \right], \quad (1)$$

where $\langle r^2 \rangle_0 = \frac{3R_0^2}{5}$ is the mean-square radius with no deformation. β_2^2 is obtained from

$$\beta_2^2 = \frac{\langle i | [Q^{(2)} \cdot Q^{(2)}] | i \rangle}{\left[\frac{3}{4\pi} A R_0^2 \right]^2}, \quad (2)$$

with $A = Z + N$. The quadrupole operator is a sum over all nucleons with

$$Q^{(2)} = \sum_i r_i^2 Y^{(2)}(\hat{r}_i) e, \quad (3)$$

One can evaluate the numerator by inserting intermediate states $|c\rangle$

$$\begin{aligned} & \langle i | [Q^{(2)} \cdot Q^{(2)}] | i \rangle \\ &= \frac{1}{(2J_i + 1)} \sum_c \langle i | Q^{(2)} | c \rangle \langle c | Q^{(2)} | i \rangle. \end{aligned} \quad (4)$$

$|c\rangle$ are excited states that are connected by the rotational model to the ground state. For even-even nuclei with $J_i = 0$, one obtains

$$\langle i | [Q^{(2)} \cdot Q^{(2)}] | i \rangle = \sum_c B(E2, 0^+ \rightarrow 2_c^+). \quad (5)$$

An extension of these equations to protons and neutrons is discussed in [27].

These equations are usually used for protons, where the sum in Eq. (3) is restricted to protons, and the A in Eq. (2) is replaced by Z , to relate the increase in the rms charge radius to the measured $B(E2, 0^+ \rightarrow 2_1^+)$, as was done, for example, in Ref. [28]. The results for increase in the charge radii for calcium are shown in Fig. (3). The $B(E2)$ data are given in Table I. For ^{42}Ca we include the 2_2^+ state that contains about 10% of the $E2$ strength. The agreement with experiment is excellent.

The Sn-Cd isotonic charge radius shift is shown in Fig. (4). The experimental data are compared to the results of spherical DFT calculations obtained the Sv-min [21] EDF as given in the experimental papers [20], [19]. The experimental isotonic shifts are about halfway between zero and the Sv-min results. The β^2 corrections are then calculated using the experiment $B(E2)$ from [29]. When this is added to the Sv-min results, the agreement with experiment is good. The reason for the shift is simply that the $B(E2)$ for the Cd isotopes are 2-3 times larger than those for the Sn isotopes (all of the data used for Fig. (4) is provided in the supplementary material).

When deformed DFT calculations are carried out, the isotopes of calcium, cadmium and tin have an energy minimum near $\beta_2 \approx 0$ resulting in $B(E2)$ that are small compared to experiment. Zero-point fluctuations around these small β_2 are required to obtain $B(E2)$ that are closer to experiment. Ref. [30] includes fluctuations with the five-dimensional collective Hamiltonian (5DCH), using the Gogny D1S interaction [31], [32] for the EDF. The fluctuations result in larger $B(E2)$ values for nuclei where the deformation minimum is small. Overall, this improves the agreement with the experimental $B(E2)$ for small deformations, see Fig. 11 of Ref. [30]. There is a corresponding increase in the rms charge radii that closely follows the expectation of the Bohr model. However, the 5DCH results for the calcium $B(E2)$ given in Table I do not agree with the trend in the experiment data. This may be due to inaccuracies in the EDF single-particle energies and resulting shell gaps near $N = 28$. Fayans et al. [14], discuss the zero-point fluctuations for the calcium isotopes using results from the random-phase approximation (RPA) as an addition to spherical DFT calculations. The RPA results for the calcium $B(E2)$ given in Table I are much smaller than experiment.

An alternative proposal for improving the calculated rms radii for spherical DFT calculations is the Fayans-type EDF [14], [17] where a pairing-type term is added. An advantage is that this can rather easily be applied to both even-even and odd-even nuclei. A specific Fayans-type EDF with parameters fitted to nuclear data is called Fy(Δr) [3]. The results for the calcium isotopes shown in panel (c) of Fig. (3) are in fair agreement with experiment. The Fy(Δr) results for Sn-Cd isotopic shift shown in Fig. (4) are in poor agreement with experiment. In these Fayans-type calculations there is no explicit

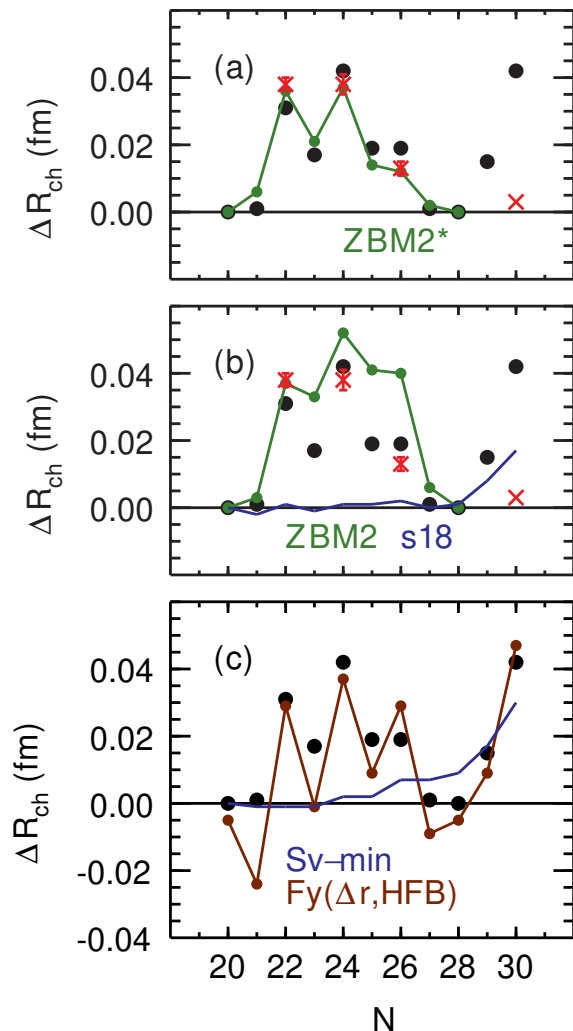


FIG. 3. ΔR_{ch} for the calcium isotopes. The black circles are the experimental results from [6] with error bars about the size of the circles. The calculations shown in panel (c) are the results from the EDF calculations with the Sv-min and Fy(Δr ,HFB) EDF as given in [18]. The red crosses in panels (a) and (b) are based on experimental $B(E2)$ values in the text. The lines shown in panels (a) and (b) are based on the $B(E2)$ calculations discussed in the text.

connection between rms radii and $B(E2)$.

For odd-even nuclei in the Bohr model there is not accurate enough experimental $B(E2)$ data for the intermediate states of Eq. (4). Also, 5DCH calculations have not been made for odd-even nuclei. An alternative is to carry out configuration-mixing (CI) calculations which can be applied to the $B(E2)$ for both even-even and odd-even nuclei. The minimal requirement is that such calculations reproduce experimental data for the $B(E2)$ in even-even nuclei.

The large experimental $B(E2)$ for $^{42,44,46}\text{Ca}$ cannot

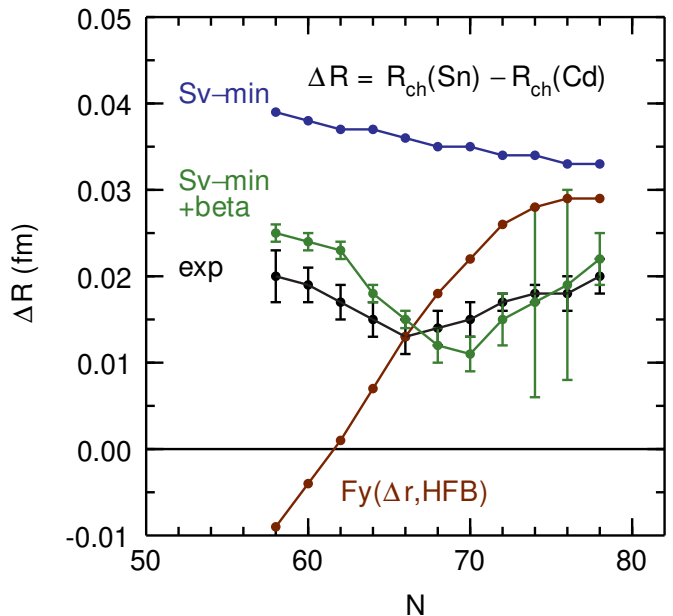


FIG. 4. Cd-Sn isotonic shifts. The experimental results from [20], and [19] are compared to the Sv-min and Fr(Δr) EDF calculations given in [20] and [19].

be described by calculations in the fp model space [36]. They are a result of admixtures from configurations with proton excitations from the sd shell to the pf shell. The CI calculations that include these cross shell excitation are challenging. In [15] the ZBM2 Hamiltonian for the $(1s_{1/2}, 0d_{3/2}, 0f_{7/2}, 1p_{3/2})$ model space was used to calculate the rms charge radii of the calcium isotopes using harmonic-oscillator radial wavefunctions. The number of protons excited from $(1s_{1/2}, 0d_{3/2})$ to $(0f_{7/2}, 1p_{3/2})$ showed an odd-even effect. When these orbital occupations were used with harmonic-oscillator radial wavefunctions one obtained an increase in the rms charge radii with odd-even oscillations that were in qualitative agreement with experiment. However, in [37] when the monopole orbital occupation numbers from these calculations were used to constrain the spherical EDF calculations, the increase in the rms charge radii was small compared to experiment. An example from [37] are the results from the $s18$ EDF shown in panel (b) of Fig. (3). The $s18$ EDF is taken from [38], and is typical of group (A) of Skyrme-type EDF shown in Fig. 5 of [37] which have effective masses of $m^*/m = 0.7 - 0.8$. Results are also shown in Fig. 5 of [37] for another group (B) of Skyrme-type EDF which have $m^*/m \approx 1.0$. The calculated kink in the rms radii at $N = 28$ depends on the effective mass. These results for group (A) are in better agreement with experiment.

To explore the β_2^2 contributions to the charge radii we will use the ZBM2-modified Hamiltonian for the

TABLE I. $B(E2 \uparrow)$ for the calcium isotopes in units of $e^2 \text{fm}^4$. For those with (a), the $B(E2)$ includes the sum for the first two 2^+ states with the details shown in Fig. (5).

N	exp	5dch [30]	RPA [14]	ZBM2	ZBM2*
22	494(23)[14](a)	466	53	440(a)	433(a)
24	470(21)[14]	601	71	624(a)	455(a)
26	182(13)[14]	607	48	474	157

($1s_{1/2}, 0d_{3/2}, 0f_{7/2}, 1p_{3/2}$) model space as described in [39]. The corrections for the rms charge radii using the $B(E2)$ values from these calculations are shown by the green line in panel (b) of Fig. (3) as ZBM2. In CI calculations one must use effective charges in Eq. (3) that account for the missing admixtures from the $2\hbar\omega$ giant quadrupole configurations [40]. We use effective charges of $e_p = 1.22$ and $e_n = 0.78$ from [27]. The results for the rms charge radii shown in Fig. (3) panel (b) are in reasonable agreement with experiment. The calculated shifts are generally too large, especially $^{45,46}\text{Ca}$. For ^{46}Ca this is due to a disagreement between the calculated and experimental $B(E2)$. This can be traced to the location of the $2p - 2h$ proton intruder state that comes at 1.8 MeV in the calculations. Experimentally it is observed at 2.4 MeV [35]. ZBM2-modified Hamiltonian was designed for the region of ^{40}Ca . When it is used for the region of ^{48}Ca the proton shell gap is too small. This can be fixed by adding a monopole term to the Hamiltonian that moves the proton $2p - 2h$ state in ^{46}Ca up to 2.4 MeV. The proton $2p - 2h$ state in ^{48}Ca is suggested to be at 4.28 MeV [41] compared to the calculated excitation energy of 4.45 MeV. The results for the β_2^2 correction are shown by the green line in panel (a) of Fig. (3) as ZBM2*. The results up to ^{48}Ca are in excellent agreement with experiment. In this model we see an example of how the rms charge radii can be related to detailed changes of structure.

The odd-even oscillation in the rms charge radii reflects the odd-even oscillations β_2^2 . The odd-even oscillations in β_2^2 can be interpreted as a blocking effect of the odd-neutron on the deformation compared to that of the neighboring even-even nuclei. In Fig. (5) details of the calculations for the $B(E2)$ compared to experiment for $^{42-45}\text{Ca}$ are shown. The energy and fragmentation of the $E2$ strength in $^{42,44}\text{Ca}$ differs from experiment, but the total is consistent with experiment. The Hamiltonian in the ($1s_{1/2}, 0d_{3/2}, 0f_{7/2}, 1p_{3/2}$) model space needs to be improved with regard to this level of detail. There is fragmentation of strength in ^{43}Ca that agrees with experiment within the uncertainties. There is also fragmentation in ^{45}Ca , but there is no data to compare with.

The difference in mirror rms charge radii is highly correlated with the symmetry energy parameter L with spherical DFT [43] and CODF [44] calculations. This was applied to recent data for rms ^{54}Ni and ^{54}Fe [27]. Due to the low-lying 2^+ state in ^{54}Ni and ^{54}Fe , β_2^2 corrections to the rms radii had to be included. When the β_2^2 correc-

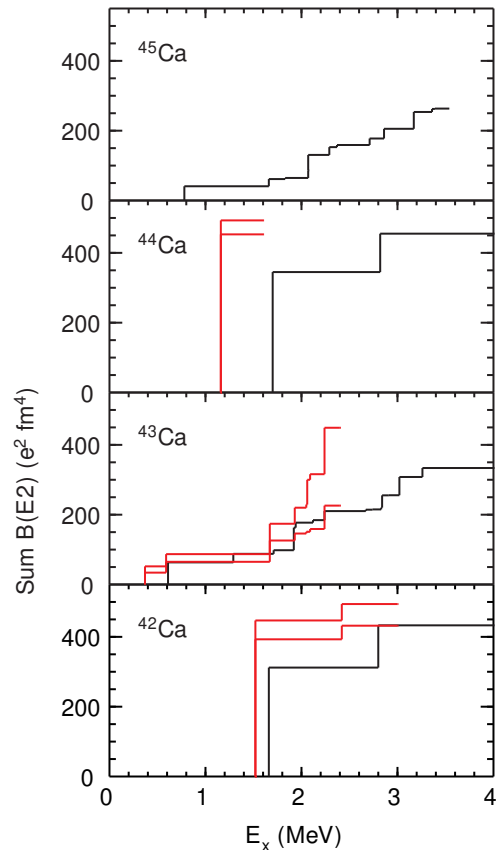


FIG. 5. Summed $B(E2, \uparrow)$ strengths in $^{42-45}\text{Ca}$ where ZBM2* results (in black) are compared with the experimental upper and low limits (in red). The experimental data are from [33] for ^{42}Ca , [42] for ^{43}Ca and [34] for ^{44}Ca .

tions are replaced by the $\text{Fy}(\Delta r)$ EDF it was shown in [45] that some of correlation between the mirror charge radii and L is lost [45].

As observed in Fig. (3), spherical EDF with our β_2^2 corrections do not account for the rapid increase observed in the rms charge radii just after $N = 28$. As discussed above, the kink at the magic numbers are correlated with the effective mass in the EDF. But the existing Skyrme EDF can only account for about half of the increase in the rms radii when one neutron is added after the magic numbers. The reason for this needs to be explored. It is noted in [46] that the occupation of the $1p_{3/2}$ orbital is

associated with a sudden change in the octupole instabilities via its large $B(E3)$ value with the $0g_{9/2}$ orbitals that differ by $\Delta j = 3$. The β_3^2 octupole contributions to rms radii in an EDF model that includes octupole degrees of freedom [46], [47] needs to be explored. Or perhaps the present generation of EDF are insufficient to take into account the sudden change in central density associated with the node in the $1p_{3/2}$ orbital. This idea was explored in [48] to qualitatively understand the increase in radii. The kinks for higher magic numbers are also associated with the addition of one neutron to an orbital with a node: $N = 50$ ($1d_{5/2}$), $N = 82$ ($1f_{7/2}$) and $N = 126$ ($1g_{9/2}$).

The kink at $N = 126$ has been widely discussed (see [49] and references therein). Most of the previous discussions have focused on the $^{210-208}\text{Pb}$ shift that depends on the DFT results for the mixing of the $1g_{9/2}$ and $0i_{11/2}$ orbitals in ^{210}Pb from pairing. However, one should first focus on the $^{209-208}\text{Pb}$ shift comes only from the occupation of one neutron in the $1g_{9/2}$ orbital.

In this letter we considered the β_2^2 corrections to rms radii provided by the Bohr model for the calcium isotopes and the cadmium-tin isotonic shifts. We showed that the experimental $B(E2)$ values can account for the rms data for even-even nuclei. For the odd-even calcium isotopes we used CI models to evaluate β_2^2 for both even-even and odd-even nuclei. The odd-even oscillations are accounted for by this method. The rapid increase in the observed charge radii after $N = 28$ are not accounted for. We suggest additions to DFT calculations that need to be explored.

This work was supported by NSF grants PHY-2110365 and PHY 2111185.

-
- [1] M. Kortelainen, Z. Sun, G. Hagen, W. Nazarewicz, T. Papenbrock, and P.-G. Reinhard, Phys. Rev. C **105**, L021303 (2022).
- [2] U. C. Perera, A. V. Afanasjev, and P. Ring, Phys. Rev. C **104**, 064313 (2021).
- [3] P.-G. Reinhard and W. Nazarewicz, Phys. Rev. C **95**, 064328 (2017).
- [4] P.-G. Reinhardt and W. Nazarewicz, Phys. Rev. C **103**, 053310 (2021).
- [5] I. Angeli, Atomic and Nuclear Data Tables **87**, 185 (2004).
- [6] R. F. Garcia Ruiz, Nature Physics **12**, 594 (2016).
- [7] L. Zamick, Ann. of Phys. (N.Y.) **66**, 784 (1971).
- [8] H. D. Wohlfahrt, E. B. Shara, M. V. Hoehn, Y. Yamazaki and R. M. Steffen, Phys. Rev. C **23**, 593 (1981).
- [9] I. Talmi, Nucl. Phys. A **423**, 189 (1984).
- [10] D. Zawischa, Phys. Legg. B **155**, 309 (1985).
- [11] F. Barranco and R. A. Broglia, Phys. Lett. B **151**, 90 (1985).
- [12] L. Zamick, Zeit. fur Phys. A **327**, 409 (1987).
- [13] M. Horoi, Phys. Rev. C **50**, 2384 (1994).
- [14] S. Fayans, S. Tolokonnikov, E. Trykov, and D. Zawischa, Nucl. Phys. A **676**, 49 (2000).
- [15] E. Caurier, K. Langanke, G. Martinez-Pinedo, F. Nowacki and P. Vogel, Phys. Lett. B **522**, 240 (2001).
- [16] L. Zamick, Phys. Rev. C **82**, 057304 (2010).
- [17] E. E. Saperstein and S. V. Tolokonnikov, Phys. At. Nucl. **74**, 1277 (2011).
- [18] A. J. Miller et al., Nat. Phys. **15**, 432 (2019).
- [19] C. Gorges et al., Phys. Rev. Lett. **122**, 192502 (2019).
- [20] M. Hammen et al., Phys. Rev. Lett. **121**, 102501 (2018).
- [21] P. Kluepfel, P.-G. Reinhard, T. J. Buervenich, and J. A. Maruhn Phys. Rev. C **79**, 034310 (2009).
- [22] I. Angeli and K. P. Marinova, Atomic Data and Nucl. Data Tables **99**, 69 (2013).
- [23] G. Fricke and K. Heilig, Nuclear Charge Radii (Springer, Berlin Heidelberg, 2004).
- [24] K. Minamisono et al., Phys. Rev. Lett. **117**, 252501 (2016).
- [25] F. Sommer et al., to be published.
- [26] S. A. Ahmad, W. Klempt, R. Neugart, E. W. Otten, P.-G. Reinhard, G. Ulm, and K. Wendt, Nucl. Phys. A **483**, 244 (1988).
- [27] S. V. Pineda et al., Phys. Rev. Lett. **127**, 182503 (2021).
- [28] B. A. Brown, C. Bronk and P. E. Hodgson, Jour. Phys. G **10**, 1683 (1984).
- [29] B. Pritychenko, M. Birch, and B. Singh, Nucl. Phys. A **962**, 73 (2017).
- [30] J.-P. Delaroche, M. Girod, J. Libert, H. Goutte, S. Hilaire, S. Peru, N. Pillet, and G. F. Bertsch, Phys. Rev. C **81**, 014303 (2010).
- [31] J. Decharge and D. Gogny, Phys. Rev. C **21**, 1568 (1980).
- [32] J.-F. Berger, M. Girod, and D. Gogny, Comput. Phys. Commun. **63**, 365 (1991).
- [33] K. Hadynska-Klek, Phys. Rev. C **97**, 024326 (2018).
- [34] C. E. Towsley, D. Cline and R. N. Horoshko, Nucl. Phys. A **204**, 574 (1973).
- [35] W. Kutschera, B. A. Brown, H. Ikezoe, G. D. Sprouse, Y. Yamazaki, Y. Yoshida, T. Nomura and H. Ohnuma, Phys. Rev. C **12**, 813 (1975).
- [36] B. Longfellow, D. Weisshaar, A. Gade, B. A. Brown, D. Bazin, K. W. Brown, B. Elman, J. Pereira, D. Rhodes, and M. Spieker, Phys. Rev. C **103**, 054309 (2021).
- [37] D. M. Rossi et al., Phys. Rev. C **92**, 014305 (2015).
- [38] B. A. Brown and A. Schwenk, Phys. Rev. C **89**, 011307(R) (2014).
- [39] M. L. Bissell et al., Phys. Rev. Lett. **113**, 052502 (2014).
- [40] B. A. Brown, A. Arima and J. B. McGrory, Nucl. Phys. A **277**, 77 (1977).
- [41] B. A. Brown and W. A. Richter, Phys. Rev. C **58**, 2099 (1998).
- [42] <https://www.nndc.bnl.gov/ensdf/getadopted.jsp?nuc=43Ca>
- [43] B. A. Brown, Phys. Rev. Lett. **119**, 122502 (2017).
- [44] J. Yang and J. Piekarewicz, Phys. Rev. C **97**, 014314 (2018).
- [45] P.-G. Reinhard and W. Nazarewicz, Phys. Rev. C **105**, L021301 (2022).
- [46] W. Nazarewicz, P. Oleadners, I. Ragnarsson, J. Dudek, G. A. Leander, P. Moeller, R. Ruchowka, Nucl. Phys. A **429**, 269 (1984).
- [47] Y. Cao, S. E. Agbemava, A. V. Afanasjev, W. Nazarewicz, and E. Olsen, Phys. Rev. C **102**, 024311 (2020).
- [48] W. Horiuchi and T. Inakura, Phys. Rev. C **105**, 016301(R) (2020).
- [49] W. Horiuchi and T. Inakura, Phys. Rev. C **105**, 044303

(2022).